Journal of Solid State Chemistry 184 (2011) 2033–2040

Contents lists available at ScienceDirect

Journal of Solid State Chemistry

journal homepage: www.elsevier.com/locate/jssc

# A very promising piezoelectric property of $Ta_2O_5$ thin films. II: Birefringence and piezoelectricity

M. Audier [a,*], B. Chenevier [a], H. Roussel [a], L. Vincent [b], A. Peña [c], A. Lintanf Salaün [d]

[a] Laboratoire des Matériaux et du Génie Physique, UMR CNRS 5628, Minatec - INP Grenoble, 3 parvis Louis Néel, BP 257, 38016 Grenoble Cedex 1, France
[b] CIME Nanotech Minatec, Microsystèmes et capteurs, F-38016 Grenoble Cedex 1, France
[c] Institut Néel – CNRS/UJF, Dpt. Matière Condensée, Matériaux et Fonctions, F-38042 Grenoble, France
[d] L2MA, CEA LETI D2NT, F-38054 Grenoble, France

ARTICLE INFO

Available online 12 June 2011

*Keywords:*
Tantalum oxide
Piezoelectricity
Birefringence
Ceramic thin film

ABSTRACT

Birefringent and piezoelectric properties of $Ta_2O_5$ ceramic thin films of monoclinic and trigonal structures were analyzed. The birefringence, observed by reflected polarized light microscopy, yields information on thin film microstructures, crystal shapes and sizes and on crystallographic orientations of grains of trigonal structure. Such an information was considered for investigating piezoelectric properties by laser Doppler vibrometry and by piezoresponse force microscopy. The vibration velocity was measured by applying an oscillating electric field between electrodes on both sides of a $Ta_2O_5$ film deposited on a Si substrate which was pasted on an isolating mica sheet. In this case, it is shown that the vibration velocity results were not only from a converse piezoelectric effect, proportional to the voltage, but also from the Coulomb force, proportional to the square of the voltage. A huge piezoelectric strain effect, up to 7.6%, is found in the case of $Ta_2O_5$ of trigonal structure. From an estimation of the electrical field through the $Ta_2O_5$ thin film, this strain likely corresponds to a very high longitudinal coefficient $d_{33}$ of several thousand picometers. Results obtained by piezoresponse force microscopy show that trigonal grains exhibit a polarization at zero field, which is probably due to stress caused expansion in the transition monoclinic–trigonal, presented in a previous article (part I).



## 1. Introduction

In a previous paper [1] hereafter denoted by I, the crystallization of amorphous $Ta_2O_5$ thin films deposited on silicon substrates was shown to occur with the formation of a monoclinic phase mL-$Ta_2O_5$ in a temperature range of about 850–1000 °C. By slow cooling to room temperature, the monoclinic phase transforms into a trigonal $Ta_2O_5$ phase ($a = 12.713(7)$ Å, $\alpha = 28.201(0)°$, space-group $R3$). This phase transition was determined to be reversible by repeating thermal treatments in oxygen atmosphere with different cooling rates. In the present paper, we compare the results of preliminary tests on the piezoelectric properties of films of monoclinic structure and partially transformed into the trigonal phase (Section 2.2). Measurements were performed by laser Doppler vibrometry (LDV) and piezoresponse force microscopy (PFM). However, optical properties of these samples observed by reflected polarized light microscopy are first reported (Section 2.1) because the results obtained by LDV on the partially transformed film were depending on the position of the laser probe (of about 10 μm diameter) on the film surface. The result of an ultrahigh piezoelectric behavior of the trigonal $Ta_2O_5$ phase is discussed in relation to its structural characteristics described in part I.

Note that this second part is published in the same journal, to facilitate a better view of the relationship between structural and physical properties of $Ta_2O_5$ structures.

## 2. Results

### 2.1. Birefringence

In this section the birefringence properties are studied and results will be considered for interpreting piezoelectric properties presented in the next section.

Through the monoclinic-to-trigonal transformation, the tantalum oxide thin film remains transparent. In this case, a property of birefringence could be verified by reflected polarized light microscopy (Leica DMLM and Zeiss Axioskop 40). The incident polarized light goes through the transparent film and is reflected at the film–silicon interface. To comply with birefringence, the optical character of the trigonal phase must be uniaxial and the

* Corresponding author. Fax: +33 456529301.
*E-mail address:* Marc.Audier@grenoble-inp.fr (M. Audier).

0022-4596/$ - see front matter © 2011 Elsevier Inc. All rights reserved.
doi:10.1016/j.jssc.2011.06.002

optic axis is parallel to the three-fold axis. The shape of the indicatrix (or refractive index ellipsoid) is a rotation ellipsoid [2].

Fig. 1(a) shows a low magnification image with crossed polarizers in vertical and horizontal positions (as indicated in insert). Crystal grains of trigonal phase whose optic axis (or a projection of their optic axis) is in the image plane and at 45° from both polarizers are illuminated. A flattened circular ellipsoid shape of grain embedded in the monoclinic phase can be inferred from the elliptical shape of their sections. As the tantalum oxide film thickness is 0.067 μm, i.e. very small compared to the size of ellipsoidal crystal grains (about 7 and 20 μm for the ellipsoidal axes), individual thin slices of ellipsoidal crystal grains are therefore observed.

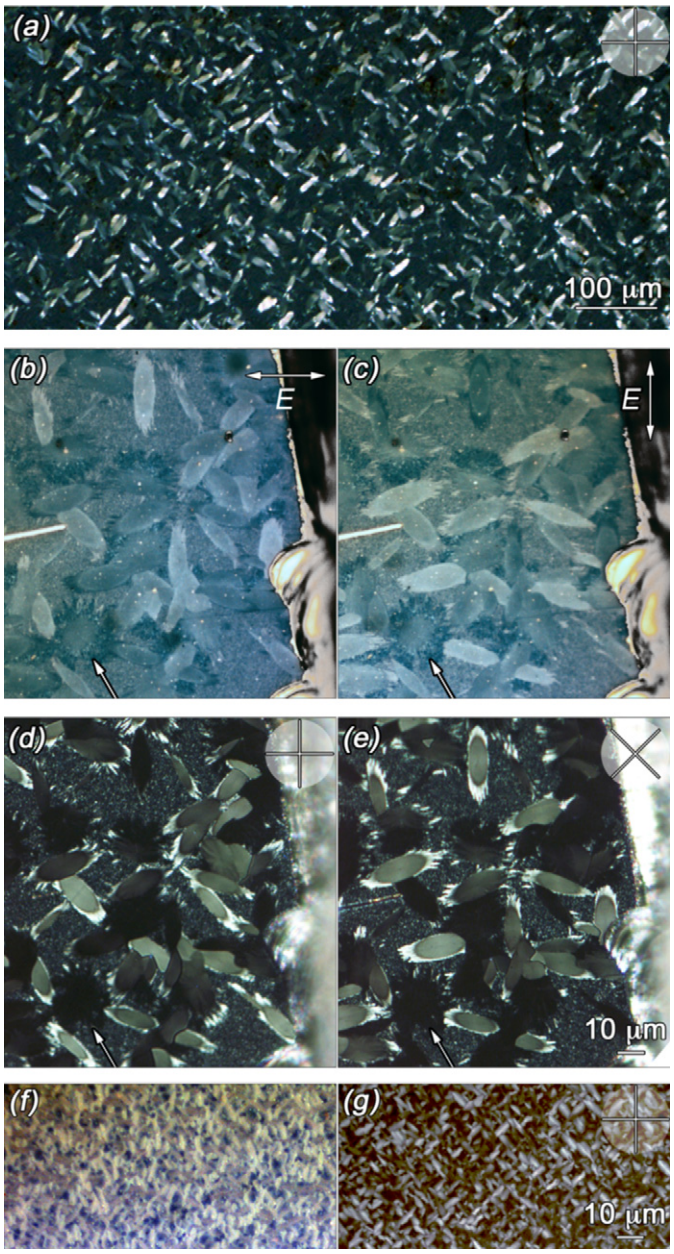


**Fig. 1.** (a–e) Images of polarized light microscopy of ellipsoidal crystal grains of trigonal structure exhibiting {111} lamellae of trigonal phase which have grown along a long axis of ellipse. Grains are embedded in a remaining monoclinic phase. (a) Low magnification image with crossed polarizers orientations indicated in inserts; (b to e) images corresponding to a same area of sample for different conditions of polarization (see text); (f and g) bright field image and corresponding crossed-polarized image related to a $Ta_2O_5$ film of monoclinic structure obtained by ESD and after the thermal treatments tt1+tt2 as indicated in Table 1 of part I.

Using only one polarizer on the reflected light, the optic axis can be identified as corresponding to the small axis of ellipsoids (Fig. 1(b, c)). For instance, the slice of ellipsoidal grain observed in the upper part of both images (b) and (c) appears respectively illuminated for an horizontal orientation of the polarizer and dark for a vertical orientation. The optical axis of this single crystal grain (or a projection of its optical axis in the image plane) is therefore in horizontal orientation. The growth of {111} lamellae of trigonal structure being normal to the optic axis (cf. part I), they appear here as small dendrites oriented along the long axis of ellipses.

The grain indicated by arrows on images (b) and (c) exhibits a circular cross-section. As its contrast does not change with a rotation of the polarizer, one can assumed that its optical axis is normal to the image plane. Using crossed polarizers, it was checked that such a grain remain black (i.e. invisible) whatever the angular orientation of the crossed polarizers, i.e. in agreement with an optic axis normal to the image plane (arrows in Fig. 1(d, e)). The light speckle observed in between ellipsoidal grains can, a priori, be attributed to the remaining monoclinic phase as it could be detected from X-ray diffraction pattern analysis (Fig. 6 in part I). Actually, birefringence resulting from the monoclinic phase has also been observed. For instance, Fig. 1(f, g) shows a bright field image and a corresponding crossed-polarized image, related to a $Ta_2O_5$ film of monoclinic structure obtained by ESD and after both thermal treatments tt1+tt2 (Table 1 in part I). We have also observed that the size and shape of illuminated domains in crossed-polarized images of pure monoclinic films changed upon variations of crystallization conditions of amorphous films. Their aspect evolves between an homogenous light speckle and elongated illuminated domains of about 10 μm length. But further experiments will be required in order to determine what structural changes are occurring in relation with different crossed-polarized images.

### 2.2. Piezoelectricity

#### 2.2.1. Laser Doppler vibrometry

Measurements by laser Doppler vibrometry were performed using a LDV Polytec OFV-3001/502, on the samples prepared by i-MOCVD and previously observed by polarized light microscopy. The LDV apparatus is constituted of an heterodyne interferometer measuring the velocity and the direction of the displacement under an alternative electrical field [3–5]. Depending on the distance between the laser head to the sample, the size of the laser probe normal to the sample surface is about 10–15 μm. It is comparable to the grain sizes of trigonal phase observed in Fig. 1.

In the case of the thin film partially transformed into trigonal phase, a gold film was deposited by evaporation on a surface of $10 \times 12$ mm$^2$ on a sample of surface $12 \times 14$ mm$^2$. The $Ta_2O_5$ film of 67 nm thickness is in contact with a $SiO_2$ layer of 8 nm thickness (insert of Fig. 1(b) in part I), itself on a (001)Si wafer of 0.6 mm thickness. This sample was sticked with cyanoacrylate glue on a mica sheet of 0.10 mm thickness and the whole was sticked on a thick and large metallic plate ($90 \times 90 \times 5$ mm$^3$) of Al alloy. Electrical contacts on each electrode were realized with a silver paste (Fig. 2(a,b)). A similar mounting was used for the thin film of monoclinic structure but with a smaller surface of gold electrode ($4 \times 4$ mm$^2$).

Such a layer stacking is obviously not appropriated for measuring a piezoelectric property as it requires to apply high electrical voltage in order to obtain a small electrical field through the tantalum oxide film.[1] The various capacitances and resistances

[1] Let us recall that the initial objective for depositing $Ta_2O_5$ thin films on silicon substrates was to study their dielectric properties [6–8] and not their piezoelectricity. Therefore, such samples were used for preliminary tests before envisaging new sample preparations dedicated to a full analysis of piezoelectric characteristics.

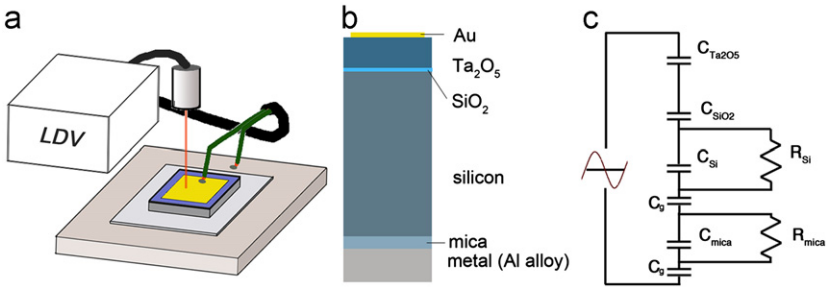


**Fig. 2.** (a) Mounting of the sample for LDV measurements and (b) stacking of layers between electrodes with (c) its equivalent electrical circuit.

**Table 1**
Estimated capacitances and resistances of the different layers shown in Fig. 2(c).

| Layer | Thickness (m) | $K$ [12] | $C^a$ | $R$ |
|---|---|---|---|---|
| Cyanoacrylate | $5\times10^{-6}$[b] | 3.3 | 701 pF | |
| Mica | $10^{-4}$ | 6 | 64 pF | 10 M Ω |
| Cyanoacrylate | $5\times10^{-6}$[b] | 3.3 | 701 pF | |
| Si[c] | $6\times10^{-4}$ | 10 | 17.7 pF | 60 Ω |
| $SiO_2$ | $8\times10^{-9}$ | 3.9 | 518 nF | |
| $Ta_2O_5$ | $67\times10^{-9}$ | 10[b] | 159 nF | |

[a] $C=K\varepsilon_0 A/d$, $\varepsilon_0\approx 8.85\times10^{-12}$ F m$^{-1}$ and $A=1.2\times10^{-4}$ m$^2$.
[b] Assumed values.
[c] B-doped silicon at a concentration of about $10^{-14}$ [13].

must be determined in order to estimate the value of the electrical field from an equivalent electrical circuit (Fig. 2(c) and Table 1). Besides, as a result of the compressive Coulomb's force ($F_C$) between the electric charges of the capacitor plates, an additional strain effect must be considered. The strain amplitude due to this force depends on the different compressive modulus of elasticity ($\sum E_C$) of the layers in between the capacitor plates.

Under an oscillating electrical field, the strain variation due to a converse piezoelectric effect can however be distinguished from this due to the Coulomb force. If the frequency of the piezoelectric strain variation must be equal to this of the oscillating electrical field, a double frequency must be observed for a strain variation due to the Coulomb force because this force is always attractive whatever the direction of the electrical field. The Coulomb force ($F_C$) between the plates of a plane capacitor can be derived from the electrostatic pressure:

$$P=\frac{1}{2}\sigma E$$

$\sigma$ is the charge density and $E$ a uniform electrical field inside the capacitor.

$F_C$ acts to reduce the distance $h$ between the plates. $F_C$ and hence the strain $\Delta h/h$ are proportional to the square of the voltage:

$$F_C=-PS=\frac{\Delta h}{h}S\sum E_C=-\frac{1}{2}\frac{CU^2}{h} \quad (1)$$

where the capacity $C=K\varepsilon_0 S/h$. $S$ is the surface of the plates, $K$ the relative dielectric constant and $\varepsilon_0$ the permittivity of free space ($\varepsilon_0\approx 8.85\times 10^{-12}$ F m$^{-1}$).

On account of a strain variation linear with $U$ for the converse piezoelectric effect and an applied ac voltage $U=U_0\sin(\omega t)$, the overall velocity of vibration ($dx/dt$) measured by LDV varies as

$$\frac{dx}{dt}=V_0^P\sin(\omega t+\phi_P)+V_0^C\sin(2\omega t+\phi_C)+cte \quad (2)$$

where $V_0^P$ and $V_0^C$ correspond to the maximal velocities of vibration for the piezoelectric and Coulomb effects respectively. The constant term in this equation has to be attributed, a priori, to an electronic noise of the photodiode used for the velocity measurement.

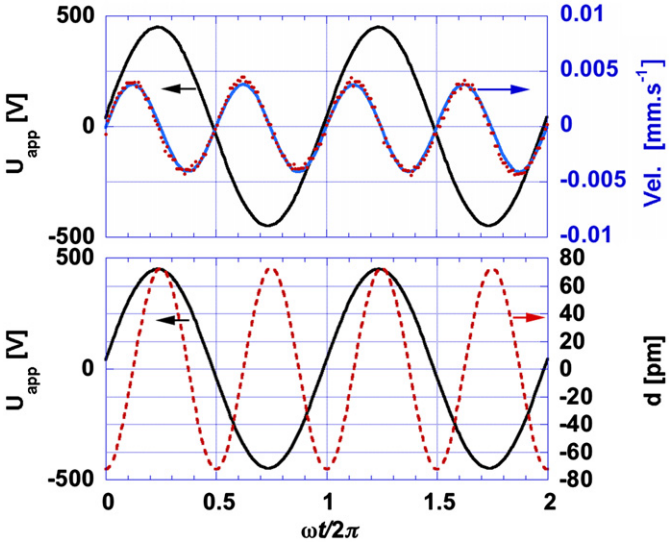


**Fig. 3.** Effect of the Coulomb force: (a) variation of the vibration velocity related to this of the applied ac voltage and (b) corresponding variation of the displacement related to this of the applied voltage $U_0$=416 V at 9.09 kHz.

Equations for the velocity variations $V_P$ and $V_C$ and values of phase shifts $\phi_P$ and $\phi_C$ can be determined by curve fitting. Both types of displacements are then calculated from the integral equations:

$$x_P=-\frac{V_0^P}{\omega}\cos(\omega t+\phi_P)=d_0^P\cos(\omega t+\phi_P) \quad (3)$$

$$x_C=-\frac{V_0^C}{2\omega}\cos(2\omega t+\phi_C)=d_0^C\cos(2\omega t+\phi_P) \quad (4)$$

As the Coulomb force remains attractive when the polarization is reversed, the displacement per volt is double (i.e. 2 $d_0^C$ for a half period of the applied voltage).

Piezoelectric strain–applied voltage hysteresis can also be plotted knowing the phase shift $\phi_P$.

### 2.2.2. Vibration resulting from the coulomb force

For this test, a gold electrode was deposited by evaporation onto a surface of about 1 cm$^2$ of a silicon wafer. This piece of Si wafer was sticked on a mica sheet, itself sticked onto the electrode of Al alloy. An ac voltage of $U_0$=416 V at 9.09 kHz was applied between both electrodes. From Fig. 3, the frequency of the velocity of vibration is, as expected, twice that of the applied ac field. There is a small phase shift of 4.3° between the applied voltage and the measured response. After integration of the sine function obtained by curve fitting of the velocity

variation, the cosine function plot of the displacement indicates a maximal displacement of amplitude 2 $d_0^C = 144$ pm at 416 V. This variation of distance seems mainly due to a deformation of the films of cyanoacrylate glue as different amplitudes of displacement were observed for different film thickness of glue (see after).

### 2.2.3. Monoclinic $Ta_2O_5$ structure

Results of LDV measurements performed on a sample with a thin film of $Ta_2O_5$ monoclinic structure are shown in Fig. 4. The film thickness was equal to $69 \pm 0.5$ nm from a TEM observation of a cross-section specimen, i.e. about the same thickness as the film of trigonal structure (67 nm). The variation of the vibration velocity observed in (a) was obtained for an ac voltage of $U_0 = 376$ V at 9.09 kHz. Both frequency and voltage were adjusted in order to maximize the amplitude of the response. The frequency of the response is almost twice that of the applied voltage because the displacement is mainly due to the Coulomb force. Using Eq. (2), a curve fitting (in blue) of the data (red points) was obtained with a very good correlation coefficient ($R = 0.9986$[2]). Then both displacements related to converse piezoelectric effect and Coulomb force were calculated using Eqs. (3) and (4). The variations of these displacements are respectively represented by a continuous line in blue and a dotted line in red in Fig. 4(b), where it appears that the Coulomb displacement ($d_0^C = 139.41$ pm) is about ten times larger than the piezoelectric displacement ($d_0^P = 14.05$ pm).

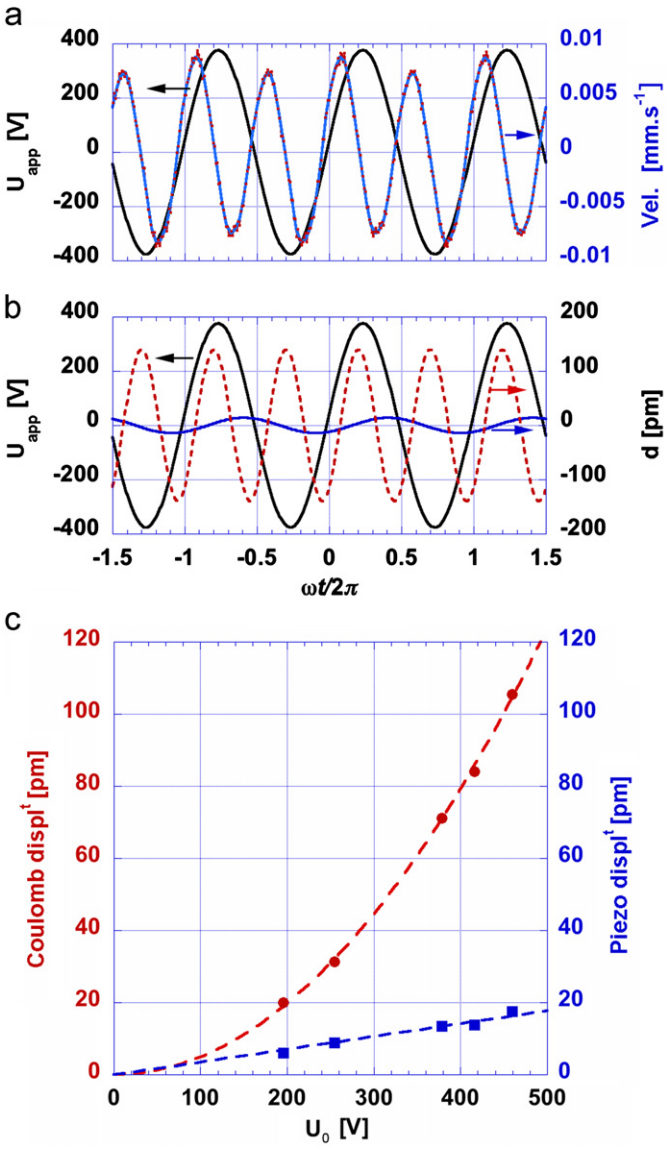


**Fig. 4.** Results of LDV measurements on a sample with a thin film of $Ta_2O_5$ monoclinic structure. (a) Variation of the measured vibration velocity related to this of an applied ac voltage of $U_0 = 376$ V at 9.09 kHz and (b) corresponding variations of piezoelectric and Coulomb displacements with their phase shifts with respect to $U_{app.}(t)$. (c) Variation laws of both piezoelectric and Coulomb displacements of the type $d_0^P = a_P U_0$ (blue dotted line) and $d_0^C = a_C U_0^2$ (red dotted line) respectively. (For interpretation of the references to color in this figure legend, the reader is referred to the web version of this article.)

LDV measurements were repeated for four other values of voltage ($U_0 = 416$ V at 9.09 kHz, 264 V at 9.01 kHz, 456 V at 9.01 kHz and 208 V at 8.93 kHz). Small changes in the frequency correspond to adjustments for maximizing the amplitude of the response. As a result, Fig. 4(c) shows that the Coulomb displacement varies according to a curve fitting $d_0^C = a_C^M U_0^2$ with $a_C^M = 0.0004945$ pm/V$^2$ in agreement with the Coulomb's law for a plane capacitor (Eq. (1)) and that the piezoelectric displacement exhibits about a linear variation $d_0^P = a_P^M U_0$ with $a_P^M = 0.03548$ pm/V for a fit passing by the origin (the superscript $M$ stands for monoclinic).

### 2.2.4. Trigonal $Ta_2O_5$ structure

Different behaviors of vibration were observed for various $x$, $y$ positions of the laser beam normal to the gold electrode surface because of the different crystallographic orientations of grains of trigonal structure, as previously observed by polarized light microscopy. But also because the $Ta_2O_5$ thin film was incompletely transformed into trigonal structure. Results corresponding to the highest variation of piezoelectric displacement that we have been observed are hereafter presented. We believe that the laser probe was in this case probably centered on a single crystal trigonal grain but of unknown crystallographic orientation. A velocity of vibration started to be observed by applying an alternative voltage of a few tens of volt in a frequency range form 50 Hz to 5 kHz. For instance, at $U_0 = 130.5$ V (or 261 V peak-to-peak) and 5 kHz, the frequency of the vibration velocity is similar to the frequency of the applied voltage (Fig. 5 column (a)). From the curve fitting (in blue) of the measured velocities (red points), both types of velocity variation, corresponding to the converse piezoelectric effect (blue line) and Coulomb force (dotted line in red) are plotted. The constant term obtained through the fitting curve procedure is here subtracted to the velocity variation due to the Coulomb force. Then the variation of each type of displacement were calculated from Eqs. (3) and (4) as well as the variation of the total displacement (black line on the last plot of column (a)). Compared to the piezoelectric displacement measured on the sample of monoclinic structure, the displacement observed on the trigonal structure is about 200 times larger. The frequency of the applied voltage was then adjusted at 3.31 kHz for which a maximal amplitude and nearly in-phase response was observed. LDV measurements were performed at three different values of $U_0$ (69, 306 and 535 V, the voltage limit of the apparatus) at 3.31 kHz (Fig. 5 columns (b–d)). The resulting plots are similar to those shown in column (a). As the voltage is increased, the part due to the Coulomb force increases more rapidly than the one due to the converse piezoelectric effect. To find a maximal amplitude of the response correspond almost to zero phase shift between $U_{app.}$ and both types of displacement. On account of the $Ta_2O_5$ film thickness of 67 nm, the piezoelectric strain at $U_0 = 535$ V is equal to a huge value of 7.64% (which might be related to the large expansion

[2] $R = \left(1 - \frac{\chi^2}{\sum_i \sigma_i (y_i - \bar{y})^2}\right)^{1/2}$ with $\chi^2 = \sigma_i \left(\frac{y_i - f(x_i)}{\sigma_i}\right)^2$.

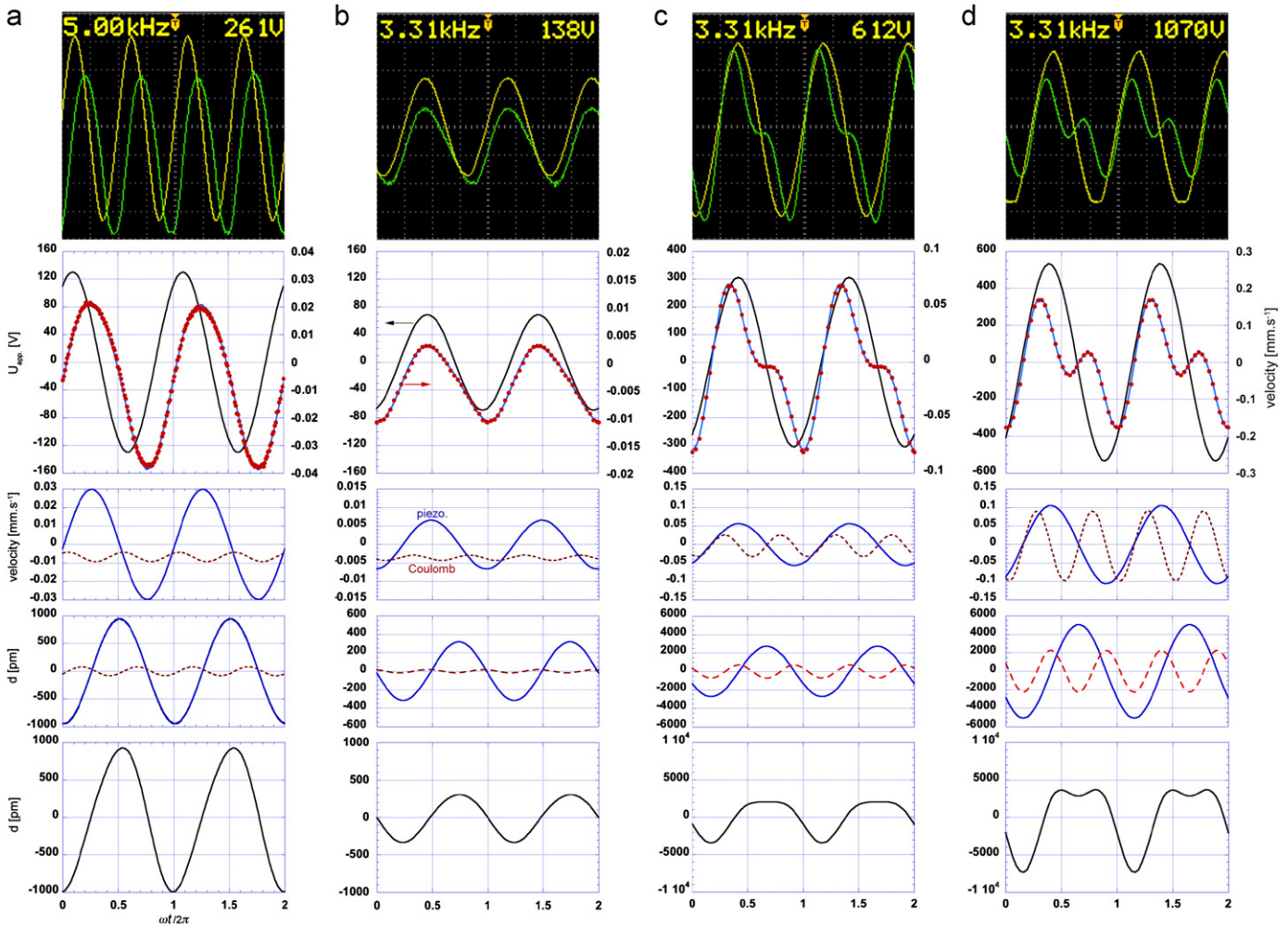


**Fig. 5.** Results of LDV measurements on a sample with a thin film of $Ta_2O_5$ trigonal structure. Column (a) shows successively an image of the screen of oscilloscope showing the variations with time of the input voltage $2U_0 = 261$ V at 5 kHz (yellow line) and of the total velocity variation (green line) and four graphs of (i) the curve fitting (in blue) of the measured velocities (red points); (ii) the velocity variations corresponding to the converse piezoelectric effect (blue line) and Coulomb force (dotted line in red) (the constant term obtained through the fitting curve procedure is here subtracted to the velocity variation due to the Coulomb force); (iii) the corresponding variations of each type of displacement and (iv) the variation of the total displacement. The presentation in columns (b, c and d) is similar to that of column (a); they correspond to results obtained at a fixed frequency of 3.31 kHz and $2U_0 = 138$, 612 and 1070 V. (For interpretation of the references to color in this figure legend, the reader is referred to the web version of this article.)

coefficient of 4.5% along the polar axis of the monoclinic–trigonal transition (see part I)).

Fig. 6(a) shows that the Coulomb displacement varies according to a curve fit $d_0^C = a_C^T U_0^2$ with $a_C^T = 0.0078555$ pm/V$^2$ and that the piezoelectric displacement exhibits a linear variation of the type $d_0^P = a_P^T U_0 - b_P^T$ with $a_P^T = 10.218$ pm/V and $b_P^T = 384.49$ pm (the superscript $T$ stands for trigonal). The coefficient for the Coulomb displacement ($a_C^T = 0.0078555$ pm/V$^2$) is here much more important than the one previously obtained for the thin film of monoclinic structure ($a_C^M = 0.0004945$ pm/V$^2$). The reason is due to thicker films of cyanoacrylate glue because an old viscous glue[3] was used to stick the sample of trigonal structure while a fresh glue (of high fluidity) was used to stick the sample of monoclinic structure. In fact, from a first LDV test on a sample of monoclinic structure prepared with an old viscous glue, the piezoelectric displacement could not be determined with a sufficient accuracy because it was less than 0.5% of the Coulomb displacement at $U_0 = 450$ V.

The origin of the constant term $b_P^T = 384.49$ pm for the linear variation of the piezoelectric displacement as a function of $U_0$, might be interpreted as a consequence of a strain resulting of the volume expansion through the monoclinic-to-trigonal transformation (see part I). On account of the film thickness of 67 nm, such a strain is equal to +0.57%; it is in between the expansion coefficient along the ternary axis (+4.5%) and the radial contraction (−1.2%). Thus, writing an equation for this strain (which is normal to the sample surface) as a combination of both expansion and contraction coefficients:

$$4.5\cos\alpha - 1.2\cos\left(\frac{\pi}{2}+\alpha\right) = 0.57$$

where $\alpha$ is the angle between the ternary axis and the normal to the surface, one obtains two solutions $\alpha = 68^\circ$ and $97.9^\circ$. In this case, the ternary optical axis of the trigonal grain would be slightly inclined of either $22^\circ$ or $7.9^\circ$ with respect to the sample surface.

Fig. 6(b) shows the corresponding piezoelectric strain–$U_{app.}$ hystereses. Their rotation is counter-clockwise. At 3.31 kHz the ellipse of hystereses have there principal axes nearly parallel to the coordinate system axes while the hysteresis is strongly

[3] As the cyanoacrylate glue used water to cure, its viscosity increases with time in the humidity of air.

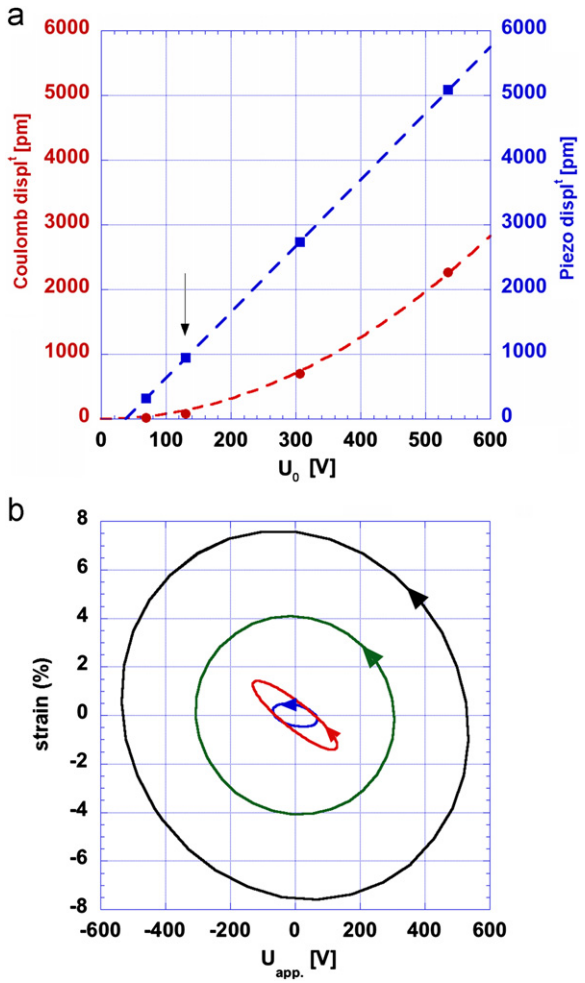


**Fig. 6.** Results of LDV measurements on a sample with a thin film of $Ta_2O_5$ trigonal structure. (a) Variation laws $d=f(U_0)$ for both piezoelectric and Coulomb displacements and (b) corresponding piezoelectric strain–$U_{app.}$ counter-clockwise hystereses. The frequency for the couple of displacement marked by an arrow was 5 kHz while it is 3.31 kHz for the three others couple of displacement. At 3.31 kHz, the ellipse of the strain–$U_{app.}$ hystereses have there minor and major axes nearly parallel to the coordinate system axes at variance with the hysteresis obtained at 5 kHz (red curve). (For interpretation of the references to color in this figure legend, the reader is referred to the web version of this article.)

flattened at 5 kHz. According to Damjanovic [9], such a dependance of the strain–voltage hysteresis as a function of frequency can be explained by a Debye-type relaxation in piezoelectric materials assumed to have defects or species that are both elastic and electric dipoles.[4] Considering a bistable model, this author demonstrates how relaxation and hysteresis in the piezoelectric properties can occur through the piezoelectric coupling of elastic and dielectric effects. As a result, the piezoelectric coefficient $d_{ij}$ has the form of complex numbers $d_{ij}=d'_{ij}-id''_{ij}$ where the imaginary part is related to energy dissipation [10]. Then for a strain given as $x=|d_{ij}|E_0\sin(\omega t-\delta)$, where $\delta$ represents the phase angle between the field and the strain, one has $\tan\delta=d''_{ij}/d'_{ij}$. As $d'_{ij}$ and $d''_{ij}$ vary with $\omega$, $\delta=90^\circ$ for $d'_{ij}=0$ and $d''_{ij}>0$ (the phase of strain is delayed 90° relative to this of the field) and the hysteresis is counter-clockwise (because $d''_{ij}>0$) with axes of ellipse parallel to the coordinate system axes. An interesting example for a similar change of the strain–voltage hysteresis with frequency but of

**Table 2**
Estimated difference of voltage $\Delta U$ and corresponding electrical fields through the tantalum oxide thin film as a function of $U_0$ (and for a film thickness of 67 nm).

| $U_0$ (V) | $f$ (kHz) | $\Delta U$ (V) | $E_0$ (V/cm) | $d_0^p$ (pm) |
|---|---|---|---|---|
| 69 | 3.31 | 0.0235 | 3507 | 318.75 |
| 130.5 | 5 | 0.045 | 6716 | 950 |
| 306 | 3.31 | 0.103 | 15373 | 2735 |
| 535 | 3.31 | 0.18 | 28358 | 5085 |

clockwise rotation is demonstrated by Damjanovic using data of Yamaguchi and Hamano [11] on the piezoelectric compound $AgNa(NO_2)_2$.

### 2.2.5. Estimation of electrical field values

Electric fields ($E$) through the tantalum oxide thin film were calculated as a function of the applied voltage $U_0$ using dielectric and resistances values from Refs. [12,13] (Tables 1 and 2). As the dielectric constant of the trigonal phase is not known, we have assumed a dielectric value of $\varepsilon_r=10\ \varepsilon_0$ determined by capacitance–voltage spectroscopy on a monoclinic $Ta_2O_5$ film.[5] The computer program LT SPICE IV [14] was used. On account of the constant of $-384.49$ pm at $U_0=0$, a plot of the displacement as function of the electrical field showed a linear variation with a slope $d_{33}=30325$ pm/V. Let us note that the electrical field through the $Ta_2O_5$ film is approximately proportional to inverse of the relative dielectric value $K$ of the film. Thus the value of $d_{33}$ is divided by a factor of about 10 for $K=1$, but which correspond to the dielectric value of vacuum!

We have also estimated the electric field in the case of the thin film of monoclinic structure for $K=10$. As a result the longitudinal coefficient $d_{33}=93$ pm/V, i.e. about 300 times less than the coefficient value of the trigonal phase.

### 2.2.6. Piezoresponse force microscopy

The tantalum oxide film on its (001)Si substrate was also observed by piezoresponse force microscopy (scanning probe microscope with a NanoScope V and using a scanning tip NSC35/TiPt) [15]. A metal electrode was pasted on the Si backside with a silver lacquer. Phase, amplitude and topography PFM images of slices of ellipsoidal trigonal grains embedded in the monoclinic phase were revealed by lateral PFM in contact mode with ac bias voltage amplitude and frequency of 10 V and 10 kHz.

The phase images in Fig. 7(a) and (b) have been taken with a dephasing of 180°, which produce a response inversion of the different zones. Corresponding amplitude and topography images are shown in (c) and (d) respectively. The topography image reveals a flat surface. The sample area analyzed by PFM was also observed by optical microscopy in order to verify characteristics of the observed phases and grains (Fig. 7(c)). Using crossed polarizers, we have determined that the monoclinic phase correspond to the zones of clear contrast on the image (a) (and respectively of dark contrast in (b)). Three crystal grains marked with a star were identified with a polar axis nearly normal to the image plane while the other grains exhibited a component of their optic axis lying in the image plane. However, any contrast variation as a function of the crystallographic orientation of grains is not observed on the PFM images. Besides, as through a dephasing of 180° the amplitude image was almost invariant, we have verified that a similar image was also obtained in non-contact mode and without ac field. Therefore, it confirms that a

[4] Damjanovic recalls however in his paper that other reasons for a piezoelectric relaxation have been proposed by different authors.

[5] Measurements made in the framework of an European IST Research project No. 10541 tantalum pentoxide photo-deposition on silicon (TOPS-II).

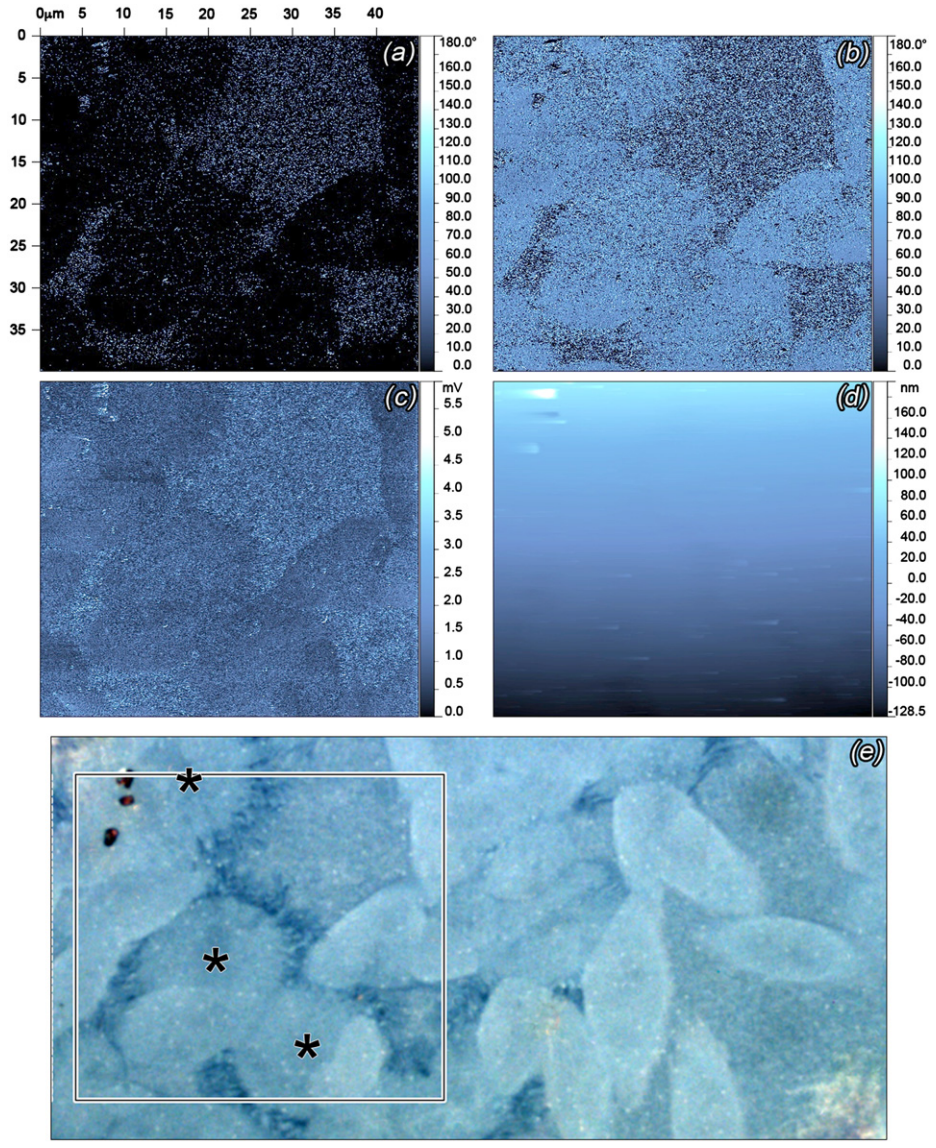


**Fig. 7.** (a, b) Lateral PFM images of the phase shift between the driving voltage and the voltage induced deformation (both images are related by a dephasing of 180°); (c, d) corresponding amplitude and topography images; (e) image of optical microscopy showing the area observed by PFM where grains of polar axis about normal to the image plane are marked with a star.

polarization of trigonal grains results of a stress induced by the volume variation of the monoclinic to trigonal phase transformation. By switching off the ac field, the amplitude image remained almost invariant because the estimated applied ac electrical field through the tantalum oxide film is about 3 mV/67 nm and appears negligible compared to the field induced by this stress (60 mV/67 nm from the previous results obtained by LDV).

## 3. Discussion and conclusion

The present results show that a new trigonal structure of tantalum oxide presents probably a very interesting piezoelectric property. Strains' variations up to $\pm 7.6\%$ have been measured under ac electric field. Assuming a dielectric value of $\varepsilon_r = 10\ \varepsilon_0$, the longitudinal piezoelectric coefficient ($d_{33}$) would be of about 30 000 pm/V while a (reasonable) value of 93 pm/V is obtained for a film of monoclinic structure. Although further works have to be undertaken to fully characterize this property, it has been already noted in a previous paper (part I) that some crystallographic aspects of this phase appeared to be in favor of a strong piezoelectricity. The preliminary results on piezoelectric measurements show that an electric polarization is partly or entirely induced by a stress resulting of a volume expansion through the monoclinic-to-trigonal phase transformation. Although this polarization can be reversed by the application of an ac electric field, we do not yet know if a spontaneous polarization at zero field, characteristic of a ferroelectric phase can occur in an unstressed state.

## Acknowledgments

One of us (M.A.) is indebted to Michel Duneau (CPHT, Ecole Polytechnique de Palaiseau) for his remark on the influence of the Coulomb's force in ac electrical field and for very fruitful discussions.

## References

[1] M. Audier, B. Chenevier, H. Roussel, L. Vincent, A. Peña, A. Lintanf Salaün, J. Solid State Chem., Part I in this issue.

[2] Th. Hahn (Ed.), International Tables for Crystallography, vol. A, Reidel, Dordrecht, 1983.
[3] C. Rembe, R. Kant, R.S. Muller, Proc. SPIE 4400 (2001) 12737.
[4] R. Prislan, Laser Doppler Vibrometry and Modal Testing, University of Ljubljana 〈www.fiz.uni-lj.si〉, 1 April 2008.
[5] S. Shinohora, A. Mochizuki, H. Yoshida, M. Sumi, Appl. Opt. 25 (1986) 9.
[6] A. Lintanf-Salaun, A. Mantoux, E. Blanquet, E. Djurado, J. Electrochem. Soc. 156 (2009) H311–H315.
[7] A. Lintanf-Salaun, Dépots par ESD et ALD et caractérisations physico-chimiques de couches d'oxydes á l'échelle nanométrique pour la microélectronique, Thesis, INP-Grenoble, 2008.
[8] Q. Fang, J.-Y. Zhang, Z.M. Wang, J.X. Wu, B.J. O'Sullivan, P.K. Hurley, T.L. Leedham, H. Davies, M. Audier, C. Jimenez, J.-P. Senateur, I.W. Boyd, Thin Solid Films 428 (2003) 242–248.
[9] D. Damjanovic, in: I. Mayergoyz, G. Bertotti (Eds.), The Science of Hysteresis, vol. 3, Elsevier, 2006.
[10] R. Holland, IEEE Trans. Sonics Ultrason. SU-14 (1967) 18.
[11] T. Yamaguchi, K. Hamano, J. Phys. Soc. Jpn. 50 (1981) 3956.
[12] 〈http://www.asiinstr.com/technical/Dielectric%20Constants.htm〉; 〈http://www.clippercontrols.com/443/pages/dielectric-constant-values〉; 〈http://physics.info/dielectrics/〉.
[13] 〈http://www.el-cat.com/silicon-properties.htm〉.
[14] LT SPICE IV (Simulation Program with Integrated Circuit Emphasis) originally developed at the Electronics Research Laboratory of the University of California, Berkeley, 1975.
[15] A. Gruverman, O. Kolosov, J. Hatano, K. Takahashi, H. Tokumoto, J. Vac. Sci. Technol. B 13 (1995) 1095.